Visualisation of Neuroblastoma Growth in a *Scid* Mouse Model Using [^{18}F]FDG and [^{18}F]FLT-PET

NINA KRIEGER-HINCK[1], HEIKE GUSTKE[1], URSULA VALENTINER[1], PAL MIKECZ[2], RALPH BUCHERT[2], JANOS MESTER[2] and UDO SCHUMACHER[1]

[1]*Department of Anatomy II: Experimental Morphology and* [2]*Department of Nuclear Medicine, University Medical Center Hamburg-Eppendorf, 20246 Hamburg, Germany*

Abstract. *Background: Tumor therapy has been monitored using the metabolic indicator [^{18}F]fluorodeoxyglucose ([^{18}F]FDG). However, the nucleotide precursor [^{18}F]fluoro-thymidine ([^{18}F]FLT) is in principle more specific as it is incorporated into DNA. Thus, the [^{18}F]FDG and [^{18}F]FLT uptake by human neuroblastomas grown in Scid mice are compared in this study. Materials and Methods: Scid mice were inoculated with human neuroblastoma cells. Tumor imaging was performed with a human whole-body full-ring PET scanner. Furthermore, the tumor weight and the cell proliferation rate were determined. Results: Neuroblastomas could be visualised using [^{18}F]FDG in 40% and with [^{18}F]FLT in 70% of the cases. [^{18}F]FDG or [^{18}F]FLT uptake could not be visualised in neuroblastomas less than 1.0 g in weight. No correlation between the cell proliferation rate and tracer uptake could be detected. Conclusion: [^{18}F]FLT showed a higher uptake than [^{18}F]FDG and, therefore, might be more suitable for monitoring anticancer therapy, at least in this tumor model.*

The use of [^{18}F]fluorodeoxyglucose ([^{18}F]FDG) has opened new possibilities for monitoring the efficacy of cancer therapy, as molecular imaging of the glucose metabolism rate in tumor tissue as an early biomarker of therapeutic response is possible. These metabolic changes usually precede morphological changes detected by magnetic resonance imaging (MRI) and computed tomography (CT), thus, giving glucose uptake monitoring a distinct advantage over pure morphological techniques (1). Positron Emission Tomography (PET) with [^{18}F]FDG is currently under intensive validation in regard to numerous clinical chemotherapy protocols (2). The validation of chemotherapy using PET extends the established indication of [^{18}F]FDG PET in the diagnosis, staging and restaging of cancer (3, 4). The glucose analogue ([^{18}F]FDG) is the most widely used PET tracer. It permeates the cell membrane via the same membrane transporters as glucose (5). [^{18}F]FDG is phosphorylated by the enzyme hexokinase resulting in the metabolic product [^{18}F]FDG-6-phosphate, which is not a substrate for further metabolism in the glycolytic pathway. Thus, [^{18}F]FDG-6-phosphate is trapped within cells in proportion to their glycolytic activity (6). As tumor detection with [^{18}F]FDG has a high sensitivity (7), its application is rapidly expanding despite its limited tumor-specificity. As macrophages and cells within granulation tissues also have a high [^{18}F]FDG uptake (8, 9) this high uptake rate can be falsely interpreted as an indication of tumor tissue (7). Furthermore, inflammation-induced [^{18}F]FDG uptake in residual masses after completed therapy can also falsely indicate viable tumor tissue. Reliable differentiation between necrotic and viable residual masses is especially important clinically, because several novel therapies are cytostatic and do not implicitly lead to a decrease of the tumor volume (10).

To overcome these limitations of [^{18}F]FDG, alternative PET tracers, such as the pyrimidine nucleoside analogue ^{11}C-thymidine, have been developed, which specifically indicates DNA biosynthesis. C-thymidine is rapidly incorporated into DNA and is suitable for imaging tumor proliferation (11). However, the clinical application of ^{11}C-thymidine has been limited by its short half-life (11) and rapid *in vivo* degradation (10). In order to overcome these problems, the thymidine analogue [^{18}F]fluorothymidine ([^{18}F]FLT), was introduced as an alternative PET tracer for cell proliferation studies (12). [^{18}F]FLT is transported into the cytoplasm by the same membrane carrier as thymidine, and is intracytoplasmically phosphorylated by the S-phase-specific enzyme, thymidine kinase 1 (TK1). The product, [^{18}F]FLT-monophosphate, is trapped within the cytosol (13), at least for a period sufficiently long for PET imaging. Studies in cell cultures and animal models indicated that [^{18}F]FLT uptake accurately reflects the TK1 activity (14-16). Furthermore, several clinical studies have shown that [^{18}F]FLT is a useful tool for imaging colorectal and lung cancer (17, 18).

Correspondence to: Prof. Udo Schumacher, University Medical Center Hamburg-Eppendorf, Department of Anatomy II, Martinistrasse 52, 20246 Hamburg, Germany. Tel: +49 40 42803 3586, Fax: +49 40 42803 5427, e-mail: uschumac@uke.uni-hamburg.de

Key Words: Neuroblastoma, FDG, FLT, PET.

In some studies, [^{18}F]FLT uptake accurately reflected proliferative activity as determined by Ki-67 immunostaining, making it an ideal tool for comprehensive cancer research (19). The antibody directed against the Ki-67 antigen has been widely used to measure cell proliferation in tumors (20). The Ki-67 protein is present during all active phases of the cell cycle (G1, S, G2, as well as mitosis), but is absent from resting cells (G0), which makes it an excellent marker for the assessment of the Ki-67 labelling index in tumor diagnostics (21).

The goals of this investigation were to determine the uptake of [^{18}F]FDG and [^{18}F]FLT in human neuroblastoma grown in *scid* mice and to examine the feasibility of utilising these two compounds as a tracer for therapy monitoring. Furthermore, the uptake of [^{18}F]FDG and [^{18}F]FLT uptake was compared with tumor weight and the cell proliferation marker Ki-67.

Materials and Methods

Radiopharmaceutical preparation. [^{18}F]FDG was synthesized in a Nuclear Interface Synthesis Module using a modification of a technique described by Hamacher *et al.* (22). [^{18}F]FLT was synthesized using 3-*N*-Boc-5'-*O*-dimethoxytrityl-3'-*O*-nosyl-thymidine (ABX Advanced Biochemical Compounds, Radeberg, Germany) as precursor in a synthesis module developed in-house. The precursor reacted with the [^{18}F] fluoride ions in the presence of Kriptofix 2.2.2. phase transfer catalyser in acetonitrile at 130˚C. After subsequent hydrolysis with 1 M hydrochloric acid, [^{18}F]FLT was purified on a semi-preparative NUCLEODUR® Pyramid C18 HPLC column (Macherey-Nagel, Düren, Germany). The column was eluted with mobile phase of 7.5% ethanol in 0.015 M phosphate buffer (pH 5.5). The product had 2-5 GBq/μmol specific activity, with >99% radiochemical purity.

Animals. In this study pathogen-free male BALB/c *scid*/*scid* (*scid*=severe combined immunodeficiency) mice (n=61) aged 6-8 weeks were used. The animals were obtained from our breeding colony and maintained under sterile conditions. They were kept in filter-top cages and were provided with sterile water and food *ad libitum*. All work involving animals was approved by the local animal experiment approval committee.

Cell line. Kelly neuroblastoma cells were obtained from Prof. Dr. R. Erttmann (University Medical Center, Hamburg-Eppendorf, Germany). They were maintained under standard cell culture conditions in RPMI-1640 medium (GIBCO, Karlsruhe, Germany) supplemented with 10% fetal calf serum, penicillin and streptomycin at 37˚C in a humidified incubator with 5% CO_2, and were free of mycoplasm infection as monitored by PCR (MP Biomedicals, Eschwege, Germany). For inoculation, Kelly neuroblastoma cells were harvested by trypsinization and 5x10^6 viable cells were suspended in 1 ml cell culture medium. Each *scid* mouse was injected subcutaneously with 0.2 ml of the cell suspension between the scapulae.

[^{18}F]FDG and [^{18}F]FLT imaging. Imaging was started on day 18 after inoculation of human neuroblastoma cells. The animals were divided into two groups, [^{18}F]FDG was applied in 28 mice, [^{18}F]FLT in 29 mice. 50 MBq of either [^{18}F]FDG or [^{18}F]FLT were injected *via* the tail vein into each mouse. After tracer application, the animals were anaesthetized by intraperitoneal injection with a mixture of ketamin-rompun-sodium chloride (1% of the body wt.). The *scid* mice were placed in a rack in the PET scanner within 15 min of tracer injection (23). Dynamic PET scans were carried out for 160 min using a conventional full-ring, whole-body PET (ECAT EXACT 921/47, CTI/Siemens, Knoxville, USA).

Histology. After completion of the PET examination, animals were killed by cervical dislocation on day 20. Tumors were excised, fixed in formalin, embedded in paraffin and cut into 5.0 μm-thick sections. Paraffin sections of the tumors were rehydrated and incubated in primary mouse monoclonal antibody against the proliferation marker Ki-67 (DAKO, Glostrup, Denmark) overnight at 4˚C. After rinsing in PBS, the sections were incubated with biotinylated secondary antibody (DAKO) for 30 min at room temperature, diluted 1:200 in antibody diluent. After washing, alkaline-phosphatase complex (Vectastain ABC Kit Alkaline Phosphatase, Wertheim, Germany) was applied for 30 min. Alkaline phosphatase activity was visualized by incubation in the substrate naphthol-AS biphosphate (Sigma, Steinheim, Germany) supplemented with New Fuchsine (Sigma-Aldrich, Steinheim, Germany) for simultaneous coupling for 20 min at room temperature. Slides were then rinsed, counterstained with hematoxylin and mounted with Cystal Mount/Clarion (Biomeda, Foster City, CA, USA). For quantitative assessment of the Ki-67 immunoreactivity, a standardized method of counting 500 nuclei in one slide for each tumor was used (24). One hundred nuclei were examined in five different microscopic fields. The percentage of proliferating cells was scored.

Statistical analysis. Visual analysis of tracer uptake was performed by two independent observers by inspecting the last frame of the dynamic scan on a computer screen using a display with three orthogonal views. The following two-score was used by each observer: tumor not visible=0, tumor visible=1. For further analysis, a tumor was classified as visible if both observers had scored tracer uptake as 1. The results of the visual evaluation of tracer uptake were compared with the cell proliferation rate (Ki-67 index) and tumor weight using the Wilcoxon non-parametric test. Animals for the two groups were randomly chosen. All values are represented as mean±SEM.

Results

Visualisation of neuroblastomas with [^{18}F]FDG and [^{18}F]FLT. Results in the [^{18}F]FDG group and in the [^{18}F]FLT group are summarized in Table I and Table II, respectively. [^{18}F]FDG allowed the visualisation of 11 out of 28 neuroblastomas (39.3%) (Figure 1). In six of the remaining 17 non-visualised cases there was disagreement between the two observers. In contrast, [^{18}F]FLT allowed the visualisation of 21 out of 29 neuroblastomas (72.4%). There was disagreement between the observers in 3 of the remaining eight non-visualised cases. Thus, the use of [^{18}F]FLT appeared to be more sensitive in identifying neuroblastomas than that of [^{18}F]FDG.

Comparison between the quantitative uptake / non-uptake of [^{18}F]FDG and [^{18}F]FLT and tumor weight. No significant differences in the tumor weight between the two groups were detected (*t*-test, $p=0.4298$). The relation between [^{18}F]FDG

Table I. *Scid mice characteristics ([18F]FDG).*

Scid mouse-No.	Body weight [g]	Tumour weight [g]	Visual Interpretation of [18F]FDG uptake (observer 1)	Visual Interpretation of [18F]FDG uptake (observer 2)	Analogue	Cell proliferation rate (Ki-67 index) [%]
116-06	24.8	0.6	0	0	A	63.6
116-07	25.7	1.0	1	1	A	72.8
116-08	27.0	0.6	1	1	A	66.8
116-09	21.0	0.9	0	0	A	63.8
116-10	22.6	2.0	1	0	D	72.0
116-11	22.1	1.4	1	0	D	62.2
117-01	23.8	1.8	1	1	A	65.4
117-02	26.3	3.1	1	1	A	74.6
117-03	27.4	1.1	1	1	A	72.0
117-04	24.6	1.1	1	1	A	67.2
117-05	20.6	1.4	0	0	A	75.4
117-06	27.3	1.7	1	1	A	66.0
117-08	27.0	1.8	0	0	A	70.8
117-11	28.3	0.8	0	0	A	62.6
119-01	23.8	2.0	1	1	A	70.8
119-02	22.3	0.6	0	1	D	59.0
119-10	25.8	0.5	0	0	A	64.4
119-11	23.4	0.8	1	1	A	66.8
119-12	22.2	0.7	0	0	A	70.6
119-13	24.6	0.7	1	0	D	59.8
119-14	24.2	0.8	0	0	A	59.6
118-07	25.6	0.7	1	0	D	62.2
118-08	21.7	0.7	0	0	A	77.4
118-09	24.5	0.9	1	1	A	65.6
118-10	25.2	0.9	0	0	A	64.4
118-11	25.7	1.1	0	0	A	68.0
118-12	24.0	1.0	1	0	D	75.2
118-13	24.1	0.7	1	1	A	66.4

A=agreeing; D=dissenting; 1=visible; 0=non-visible.

and [18F]FLT uptake / non-uptake and weight is shown in Figure 2. However, the non-visualised neuroblastomas tended to be lighter than the visualised ([18F]FDG=0.98±0.10 g and [18F]FLT=0.76±0.18 g), but the differences between visualised and non-visualised were not statistically significant (*t*-test, ([18F]FDG: $p=0.1081$, [18F]FLT: $p=0.1971$).

Comparison between the quantitative [18F]FDG and [18F]FLT uptake and the cell proliferation rate. All neuroblastomas contained Ki-67 positive cells (Table I and II). The mean number of Ki-67 positive cells was similar for [18F]FDG (68.6±1.00%) and [18F]FLT (65.8±1.31%) (Figure 3). No significant correlation was found between the cell proliferation rate and the [18F]FDG score or the [18F]FLT score.

Discussion

Neuroblastomas are malignant tumors of neuroectodermal origin presenting predominantly in early childhood (25). As only about half of the patients with metastatic neuroblastomas can be cured (26), development of new therapeutic strategies for this tumor type is clinically important.

In the present study, human neuroblastomas grown in *scid* mice were imaged by [18F]FDG and [18F]FLT-PET. Whilst 39.3% of the neuroblastomas were visualised using [18F]FDG, 72.4% were visualised using [18F]FLT. The results of our study suggest that the use of in imaging provides greater [18F]FLT sensitivity compared to [18F]FDG in the detection of neuroblastomas in this *scid* mouse model. Given the results of previous studies comparing [18F]FDG and [18F]FLT-PET uptake in tumors, it was not expected that the use of [18F]FLT would provide greater sensitivity in detecting neuroblastomas than [18F]FDG, as in other tumors including esophageal cancer (5), laryngeal cancer (27), lung (28) and thoracic tumors (29, 30) [18F]FDG uptake was higher than [18F]FLT uptake. However, Chen *et al.* (31) showed that [18F]FLT is taken up more than [18F]FDG in patients with high-grade gliomas (31), as well as in those with primary breast cancer (32). Preclinical studies compared [18F]FDG and [18F]FLT uptake in radiation-induced fibrosarcoma 1 (RIF-1) tumor-

Table II. *Scid mice characteristics ([18F]FLT).*

Scid mouse-No.	Body weight [g]	Tumour weight [g]	Visual Interpretation of [18F]FLT uptake (observer 1)	Visual Interpretation of [18F]FLT uptake (observer 2)	Analogue	Cell proliferation rate (Ki-67 index) [%]
115-01	25.6	0.5	1	0	D	75.2
116-01	27.9	0.5	1	1	A	64.8
116-02	27.2	0.6	1	1	A	65.2
116-03	26.3	0.9	1	1	A	68.0
116-04	26.7	0.4	1	1	A	62.4
116-05	27.9	0.5	1	1	A	75.6
116-12	21.9	-	0	0	A	-
117-07	26.0	0.3	0	0	A	62.2
117-09	27.5	0.9	1	1	A	73.8
117-12	24.7	0.6	1	1	A	63.4
117-13	27.1	1.4	1	1	A	65.2
117-14	25.9	3.1	1	1	A	67.2
117-15	24.4	0.4	0	0	A	60.0
117-16	23.7	1.9	1	1	A	65.8
119-03	21.8	2.2	1	1	A	57.0
119-04	23.9	0.6	0	1	D	58.6
119-05	23.5	0.9	0	0	A	64.2
119-06	24.4	1.9	1	1	A	55.8
119-07	22.4	1.5	1	1	A	76.2
119-08	21.9	0.8	1	1	A	57.8
119-09	22.4	1.4	1	1	A	63.2
118-01	25.7	1.3	1	1	A	59.8
118-02	28.3	0.9	1	0	D	63.4
118-03	25.5	1.0	1	1	A	58.8
118-04	28.0	1.1	1	1	A	70.6
118-05	24.9	1.7	0	0	A	69.8
118-06	26.8	0.9	1	1	A	67.6
118-14	24.6	0.3	1	1	A	71.0
118-15	23.4	0.6	1	1	A	72.2

A=agreeing; D=dissenting; 1=visible; 0=non-visible.

bearing mice after cisplatin treatment (2), as well as in RIF-1 tumor-bearing C3H/Hej mice after 5-fluorouracil treatment (10) and found decreased [18F]FLT uptake compared to [18F]FDG uptake. Another research group monitored androgen ablation therapy in mice with implanted prostate cancer cells using [18F]FLT. [18F]FLT uptake decreased in treated mice, but in untreated mice no change in [18F]FLT uptake was seen (33). All preclinical results indicate that [18F]FLT is probably a promising tracer for evaluating anti-proliferative drug activity in oncology. The differences in the results of these studies have several causes. On the one hand, a low tissue uptake of [18F]FLT may be due to a low [18F]FLT phosphorylation rate, which *in vitro* is known to be about 30% of the phosphorylation rate of serum thymidine by TK1 (7). On the other hand, it has been reported that the serum thymidine level in rodents is ten-fold than that in humans (13). Endogenous thymidine may compete with [18F]FLT for the uptake transporter and phosphorylation by TK1, leading to lower [18F]FLT uptake in tumor cells in rodents (13). It is important to note that false-negative and false-positive [18F]FLT results have been reported by different groups (11, 30). The reasons for these observations could be the partial volume effect, different cellular density of the tumors or differences in the proliferative activity of tumor cells (11). Given these and the results of our study, performed in a *scid* mouse model, [18F]FLT may be a more cancer-specific PET tracer than [18F]FDG and [18F]FLT-PET might afford insights into the proliferative potential of neuroblastoma beyond the anatomic localisation of disease.

Tumor weight was not statistically significantly different between uptake and non-uptake of [18F]FDG and [18F]FLT. Neuroblastomas with weights below 1.0 g did not show [18F]FDG or [18F]FLT uptake, most likely because of the limited spatial resolution of the human PET system used in the present study. Conventional human PET systems provide a maximum spatial resolution of 7 mm full width at half maximum (FWHM). Tumors smaller than this cannot be imaged reliably (34). Recently, integrated PET/CT scanners have been introduced, allowing combination of anatomical details with functional information.

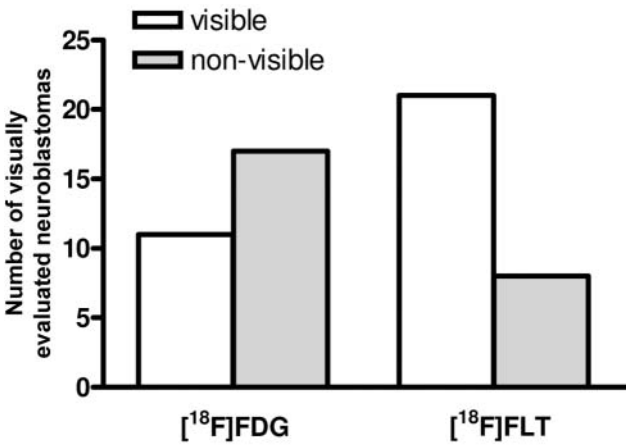

Figure 1. *Summary of the visually evaluated neuroblastomas with [18F]FDG (n=28) and [18F]FLT (n=29).*

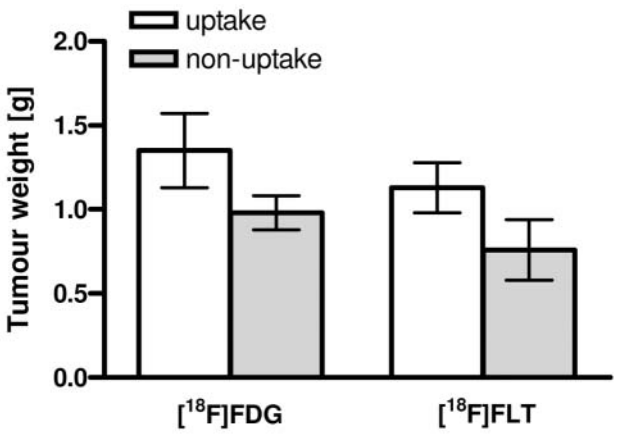

Figure 2. *Comparison of the quantitative uptake / non-uptake of [18F]FDG (n=28) and [18F]FLT (n=29) with tumour weight. Data are means±SEM.*

In addition, [18F]FDG and [18F]FLT uptake did not correlate with the Ki-67 labelling index in the current study. This result may have been due to the partial volume effect and / or inhomogeneity of the tumors (large necrotic areas in some tumors). Recent studies show a similar lack of correlation between the Ki-67 labelling index and [18F]FDG and [18F]FLT uptake in esophageal cancers (5) and in pancreatic carcinoma (35). In primary breast cancer (32) and in thoracic tumors (29), studies also revealed no association between the Ki-67 labelling index and [18F]FLT uptake. In contrast to these and our results, a correlation between the Ki-67 and [18F]FLT uptake has been described in solitary pulmonary nodules (19) and brain gliomas (31). Thus the correlation between the Ki-67 labelling index and [18F]FLT uptake seems to be dependent on the tumor itself.

In conclusion, we have shown that in the detection of neuroblastomas [18F]FLT had a higher uptake than [18F]FDG in the *scid* mouse model used in the present study. Therefore, [18F]FLT-PET might be useful for the evaluation of neuroblastomas and in monitoring anticancer therapy in this model.

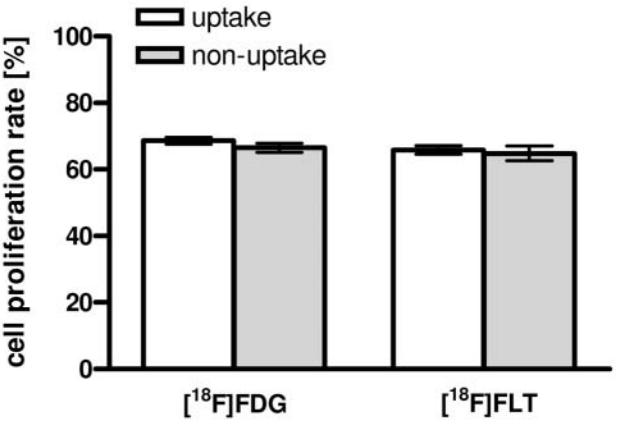

Figure 3. *Comparison of the quantitative uptake / non-uptake of [18F]FDG (n=28) and [18F]FLT (n=29) with the cell proliferation rate. Data are means±SEM.*

Acknowledgements

We thank S. Feldhaus for helping with the animals. The financial aid of the Molecular Imaging North (MOIN) programme is gratefully acknowledged.

References

1 Dose Schwarz J, Bader M, Jenicke L, Hemminger G, Janicke F and Avril N: Early prediction of response to chemotherapy in metastatic breast cancer using sequential 18F-FDG PET. J Nucl Med *46*: 1144-1150, 2005.

2 Leyton J, Latigo JR, Perumal M, Dhaliwal H, He Q and Aboagye EO: Early detection of tumor response to chemotherapy by 3'-deoxy-3'-[18F]fluorothymidine positron emission tomography: the effect of cisplatin on a fibrosarcoma tumor model *in vivo*. Cancer Res *65*: 4202-4210, 2005.

3 Hazelton TR and Coppage L: Imaging for lung cancer restaging. Semin Roentgenol *40*: 182-192, 2005.

4 Avril NE and Weber WA: Monitoring response to treatment in patients utilizing PET. Radiol Clin North Am *43*: 189-204, 2005.

5 van Westreenen HL, Cobben DC, Jager PL, van Dullemen HM, Wesseling J, Elsinga PH and Plukker JT: Comparison of 18F-FLT-PET and 18F-FDG PET in esophageal cancer. J Nucl Med *46*: 400-404, 2005.

6 Pauwels EK, Sturm EJ, Bombardieri E, Cleton FJ and Stokkel MP: Positron-emission omography with [18F]fluorodeoxyglucose. Part I. Biochemical uptake mechanism and its implication for clinical studies. J Cancer Res Clin Oncol *126*: 549-559, 2000.

7 van Waarde A, Cobben DC, Suurmeijer AJ, Maas B, Vaalburg W, de Vries EF, Jager PL, Hoekstra HJ and Elsinga PH: Selectivity of 18F-FLT and 18F-FDG for differentiating tumor from inflammation in a rodent model. J Nucl Med *45*: 695-700, 2004.

8 Kubota R, Yamada S, Kubota K, Ishiwata K, Tamahashi N and Ido T: Intratumoral distribution of fluorine-18-fluorodeoxyglucose *in vivo*: high accumulation in macrophages and granulation tissues studied by microautoradiography. J Nucl Med *33*: 1972-1980, 1992.

9 Kubota R, Kubota K, Yamada S, Tada M, Ido T and Tamahashi N: Microautoradiographic study for the differentiation of intratumoral macrophages, granulation tissues and cancer cells by the dynamics of fluorine-18-fluorodeoxyglucose uptake. J Nucl Med *35*: 104-112, 1994.

10 Barthel H, Cleij MC, Collingridge DR, Hutchinson OC, Osman S, He Q, Luthra SK, Brady F, Price PM and Aboagye EO: 3'-deoxy-3'-[^{18}F]fluorothymidine as a new marker for monitoring tumor response to antiproliferative therapy *in vivo* with positron emission tomography. Cancer Res *63*: 3791-3798, 2003.

11 Choi SJ, Kim JS, Kim JH, Oh SJ, Lee JG, Kim CJ, Ra YS, Yeo JS, Ryu JS and Moon DH: [^{18}F]3'-deoxy-3'-fluorothymidine PET for the diagnosis and grading of brain tumors. Eur J Nucl Med Mol Imaging *32*: 653-659, 2005.

12 Shields AF, Grierson JR, Dohmen BM, Machulla HJ, Stayanoff JC, Lawhorn-Crews JM, Obradovich JE, Muzik O and Mangner TJ: Imaging proliferation *in vivo* with [F-18]FLT and positron emission tomography. Nat Med *4*: 1334-1336, 1998.

13 Been LB, Suurmeijer AJ, Cobben DC, Jager PL, Hoekstra HJ and Elsinga PH: [^{18}F]FLT-PET in oncology: current status and opportunities. Eur J Nucl Med Mol Imaging *31*: 1659-1672, 2004.

14 Rasey JS, Grierson JR, Wiens LW, Kolb PD and Schwartz JL: Validation of FLT uptake as a measure of thymidine kinase-1 activity in A549 carcinoma cells. J Nucl Med *43*: 1210-1217, 2002.

15 Schwartz JL, Tamura Y, Jordan R, Grierson JR and Krohn KA: Monitoring tumor cell proliferation by targeting DNA synthetic processes with thymidine and thymidine analogs. J Nucl Med *44*: 2027-2032, 2003.

16 Toyohara J, Waki A, Takamatsu S, Yonekura Y, Magata Y and Fujibayashi Y: Basis of FLT as a cell proliferation marker: comparative uptake studies with [3H]thymidine and [3H]arabinothymidine, and cell-analysis in 22 asynchronously growing tumor cell lines. Nucl Med Biol *29*: 281-287, 2002.

17 Francis DL, Visvikis D, Costa DC, Arulampalam TH, Townsend C, Luthra SK, Taylor I and Ell PJ: Potential impact of [^{18}F]3'-deoxy-3'-fluorothymidine *versus* [^{18}F]fluoro-2-deoxy-D-glucose in positron emission tomography for colorectal cancer. Eur J Nucl Med Mol Imaging *30*: 988-994, 2003.

18 Vesselle H, Grierson J, Muzi M, Pugsley JM, Schmidt RA, Rabinowitz P, Peterson LM, Vallieres E and Wood DE: *In vivo* validation of 3'deoxy-3'-[(18)F]fluorothymidine ([(18)F]FLT) as a proliferation imaging tracer in humans: correlation of [(18)F]FLT uptake by positron emission tomography with Ki-67 immunohistochemistry and flow cytometry in human lung tumors. Clin Cancer Res *8*: 3315-3323, 2002.

19 Buck AK, Schirrmeister H, Hetzel M, Von Der Heide M, Halter G, Glatting G, Mattfeldt T, Liewald F, Reske SN and Neumaier B: 3-deoxy-3-[(18)F]fluorothymidine-positron emission tomography for noninvasive assessment of proliferation in pulmonary nodules. Cancer Res *62*: 3331-3334, 2002.

20 Heidebrecht HJ, Buck F, Steinmann J, Sprenger R, Wacker HH and Parwaresch R: p100: a novel proliferation-associated nuclear protein specifically restricted to cell cycle phases S, G2, and M. Blood *90*: 226-233, 1997.

21 Scholzen T and Gerdes J: The Ki-67 protein: from the known and the unknown. J Cell Physiol *182*: 311-322, 2000.

22 Hamacher K, Coenen HH and Stocklin G: Efficient stereospecific synthesis of no-carrier-added 2-[^{18}F]-fluoro-2-deoxy-D-glucose using aminopolyether supported nucleophilic substitution. J Nucl Med *27*: 235-238, 1986.

23 Buchert R, de Wit M, Raabe A, Bohuslavizki KH, Schulte U, Mester J and Clausen M: Low-cost, small-animal shelf for simultaneously assessing several small animals with a whole-body PET scanner. J Nucl Med Technol *28*: 171-172, 2000.

24 Sharma R, Adam E and Schumacher U: The action of 5-fluorouracil on human HT29 colon cancer cells grown in SCID mice: mitosis, apoptosis and cell differentiation. Br J Cancer *76*: 1011-1016, 1997.

25 Izbicka E and Izbicki T: Therapeutic strategies for the treatment of neuroblastoma. Curr Opin Investig Drugs *6*: 1200-1214, 2005.

26 Berthold F, Boos J, Burdach S, Erttmann R, Henze G, Hermann J, Klingebiel T, Kremens B, Schilling FH, Schrappe M, Simon T and Hero B: Myeloablative megatherapy with autologous stem-cell rescue *versus* oral maintenance chemotherapy as consolidation treatment in patients with high-risk neuroblastoma: a randomised controlled trial. Lancet Oncol *6*: 649-658, 2005.

27 Cobben DC, van der Laan BF, Maas B, Vaalburg W, Suurmeijer AJ, Hoekstra HJ, Jager PL and Elsinga PH: ^{18}F-FLT-PET for visualization of laryngeal cancer: comparison with ^{18}F-FDG PET. J Nucl Med *45*: 226-231, 2004.

28 Buck AK, Halter G, Schirrmeister H, Kotzerke J, Wurziger I, Glatting G, Mattfeldt T, Neumaier B, Reske SN and Hetzel M: Imaging proliferation in lung tumors with PET: ^{18}F-FLT *versus* ^{18}F-FDG. J Nucl Med *44*: 1426-1431, 2003.

29 Dittmann H, Dohmen BM, Paulsen F, Eichhorn K, Eschmann SM, Horger M, Wehrmann M, Machulla HJ and Bares R: [^{18}F]FLT-PET for diagnosis and staging of thoracic tumors. Eur J Nucl Med Mol Imaging *30*: 1407-1412, 2003.

30 Yap CS, Czernin J, Fishbein MC, Cameron RB, Schiepers C, Phelps ME and Weber WA: Evaluation of thoracic tumors with ^{18}F-fluorothymidine and ^{18}F-fluorodeoxyglucose-positron emission tomography. Chest *129*: 393-401, 2006.

31 Chen W, Cloughesy T, Kamdar N, Satyamurthy N, Bergsneider M, Liau L, Mischel P, Czernin J, Phelps ME and Silverman DH: Imaging proliferation in brain tumors with ^{18}F-FLT-PET: comparison with ^{18}F-FDG. J Nucl Med *46*: 945-952, 2005.

32 Smyczek-Gargya B, Fersis N, Dittmann H, Vogel U, Reischl G, Machulla HJ, Wallwiener D, Bares R and Dohmen BM: PET with [^{18}F]fluorothymidine for imaging of primary breast cancer: a pilot study. Eur J Nucl Med Mol Imaging *31*: 720-724, 2004.

33 Oyama N, Ponde DE, Dence C, Kim J, Tai YC and Welch MJ: Monitoring of therapy in androgen-dependent prostate tumor model by measuring tumor proliferation. J Nucl Med *45*: 519-525, 2004.

34 Pacak K, Eisenhofer G and Goldstein DS: Functional imaging of endocrine tumors: role of positron emission tomography. Endocr Rev *25*: 568-580, 2004.

35 Buck AC, Schirrmeister HH, Guhlmann CA, Diederichs CG, Shen C, Buchmann I, Kotzerke J, Birk D, Mattfeldt T and Reske SN: Ki-67 immunostaining in pancreatic cancer and chronic active pancreatitis: does *in vivo* FDG uptake correlate with proliferative activity? J Nucl Med *42*: 721-725, 2001.

Received May 15, 2006
Accepted July 7, 2006